

COVER PAGE

Document downloaded by @DAEL

Tue Nov 17 20:35:31 2026
For personal use

When automatic English translation is provided, only the original document is authentic.
The EAA cannot be held responsible of any translation error

Bibliographical reference

A Single Microphone Capillary-Based System for Measuring the Complex Input Impedance of Musical Wind Instruments, D. B. Sharp, A. Mamou-Mani and M. Van Walstijn, Acta Acustica **vol. 97** (Number 5), 2011, pp. 819-829

DOI
https://doi.org/10.3813/AAA.918462

Acta Acustica united with Acustica
Vol. 97 (2011) 819 – 829

DOI 10.3813/AAA.918462

A Single Microphone Capillary-Based System for Measuring the Complex Input Impedance of Musical Wind Instruments

D. B. Sharp[1)], A. Mamou-Mani[1)], M. van Walstijn[2)]

[1)] Acoustics Research Group, DDEM, MCT Faculty, Open University, Walton Hall, Milton Keynes, MK7 6AA, UK. D.Sharp@open.ac.uk

[2)] School of Electronics, Electrical Engineering and Computer Science, SARC, Queen's University, Belfast, BT7 1NN, UK

Summary

Capillary-based systems for measuring the input impedance of musical wind instruments were first developed in the mid-20th century and remain in widespread use today. In this paper, the basic principles and assumptions underpinning the design of such systems are examined. Inexpensive modifications to a capillary-based impedance measurement set-up made possible due to advances in computing and data acquisition technology are discussed. The modified set-up is able to measure both impedance magnitude and impedance phase even though it only contains one microphone. In addition, a method of calibration is described that results in a significant improvement in accuracy when measuring high impedance objects on the modified capillary-based system. The method involves carrying out calibration measurements on two different objects whose impedances are well-known theoretically. The benefits of performing two calibration measurements (as opposed to the one calibration measurement that has been traditionally used) are demonstrated experimentally through input impedance measurements on two test objects and a Boosey and Hawkes oboe.

PACS no. 4358.Bh, 43.75.Ef, 43.75.Fg, 43.75.Yy

1. Introduction

In the acoustical study of musical wind instruments, the measurement of input impedance as a function of frequency has proved particularly useful. Impedance magnitude and phase curves provide information about both the strengths and frequencies of the instrument's air column resonances. In most playing situations, it is these air column resonances, rather than the reed or lip vibrations, that control the oscillation. Consequently, impedance curves can impart a great deal of information about the playing characteristics of an instrument.

The input impedance $Z_x(\omega)$ of an air column x, such as that of a musical wind instrument, is defined as the ratio of the acoustic pressure $p_x(\omega)$ and the volume velocity $U_x(\omega)$ at the entrance to the air column,

$$Z_x(\omega) = \frac{p_x(\omega)}{U_x(\omega)}, \tag{1}$$

where ω is the angular frequency.

The input impedance, pressure and volume velocity are complex quantities so can be expressed in terms of magnitude and phase,

$$Z_x(\omega) = \left|Z_x(\omega)\right| e^{j\psi_x(\omega)}, \tag{2}$$

$$p_x(\omega) = \left|p_x(\omega)\right| e^{j\theta_x(\omega)}, \tag{3}$$

$$U_x(\omega) = \left|U_x(\omega)\right| e^{j\varphi_x(\omega)}, \tag{4}$$

where $\psi_x(\omega)$, $\theta_x(\omega)$ and $\varphi_x(\omega)$ are the phases of the input impedance, pressure and volume velocity respectively.

As the input impedance is a complex quantity, for a complete measurement both its magnitude and phase must be determined. The magnitude of the input impedance is simply the ratio of the pressure amplitude and the volume velocity amplitude,

$$\left|Z_x(\omega)\right| = \frac{\left|p_x(\omega)\right|}{\left|U_x(\omega)\right|}, \tag{5}$$

whilst the phase of the input impedance is the difference between the phases of the pressure and the volume velocity,

$$\psi_x(\omega) = \theta_x(\omega) - \varphi_x(\omega). \tag{6}$$

Since the work of Webster and Kent on cup-mouthpiece instruments in 1947 [1] and the subsequent improvements to their impedance measurement apparatus by Benade

Received 17 February 2011,
accepted 15 June 2011.

© S. Hirzel Verlag · EAA

Document downloaded by @DAEL, 2026-11-17 20:35:34 - personal use only

[2, 3], Backus [4, 5] and Caussé *et al.* [6], numerous techniques for measuring input impedance have been developed. Comprehensive reviews of methods realised in the 20th century can be found in papers by Benade and Ibisi [7] and by Dalmont [8]. Meanwhile, more recent techniques are reported in papers by van Walstijn *et al.* [9], Dickens *et al.* [10], Dalmont and Le Roux [11], Curtit *et al.* [12] and Kemp *et al.* [13]. However, despite the fact that these newer methods generally provide more accurate impedance measurements over a wider bandwidth (up to as high as around 20 kHz), many acoustics laboratories still use capillary-based experimental measurement systems similar to those documented by Benade, Backus and Caussé *et al.* These are often produced in-house but, in recent years, the commercially available BIAS system [14, 15, 16] has also achieved widespread use.

There are several reasons for the enduring popularity of capillary-based impedance measurement systems. Firstly, the apparatus can be made very compact, making it easy to transport to places such as historical instrument collections or makers' workshops. Secondly, such systems have an inherent simplicity. While newer techniques tend to require post-processing of the measured impedance to remove the effects of the coupling of the instrument to the apparatus, capillary-based systems provide a direct measurement of the impedance of the instrument itself. Finally, and perhaps most importantly, while other methods may be more accurate over a wider bandwidth, capillary-based systems still provide sufficiently accurate impedance measurements over the frequency range of interest to be useful for the study of musical wind instruments.

In the next section, the basic principles behind the design of capillary-based impedance measurement systems are described. Then, in section 3, inexpensive modifications to a capillary-based system made possible due to advances in computing and data acquisition technology are discussed. The modified set-up is able to measure both impedance magnitude and impedance phase even though it only contains one microphone. Finally, in section 4, a method of calibration is described that gives a significant improvement in accuracy when measuring high impedance objects on the modified capillary-based system. The benefits of this method are demonstrated and evaluated through input impedance magnitude and phase measurements on two test objects and a Boosey and Hawkes oboe.

2. Basic capillary-based measurement system

2.1. Introduction

The earliest capillary-based measurement systems were primarily designed to enable the measurement of input impedance magnitude, although they could also provide phase information. In such systems, the air column under test is excited using a source of volume velocity which has a constant amplitude over the frequency range of interest. From equation (5), it can be seen that the pressure amplitude is then directly proportional to the input impedance magnitude. By measuring the pressure response at the entrance to the air column, the input impedance magnitude of the air column can be deduced. As capillary-based measurement systems are generally only able to measure the plane wave component of the impedance, the excitation frequency must be kept below the cut-on frequency of the first higher mode of the air column under investigation. This ensures that all modes except the plane wave mode are nonpropagating.

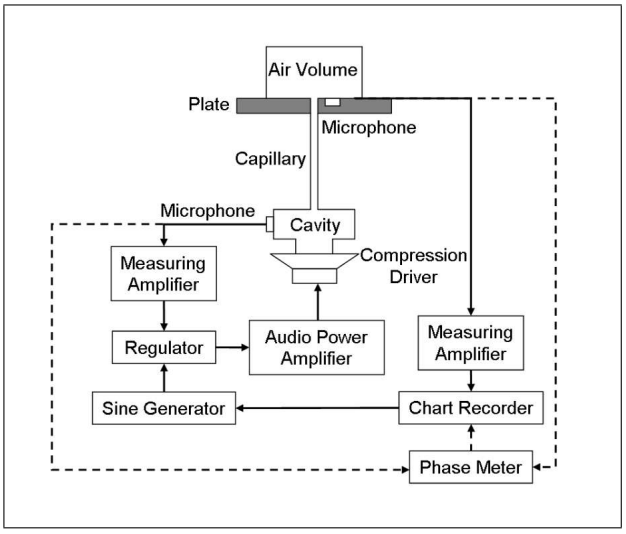


Figure 1. Dual microphone capillary-based impedance measurement set-up.

2.2. Description of measurement system

Figure 1 shows a schematic diagram of a basic capillary-based system (of the type reported in [2, 3, 4, 5, 6]) for measuring the input impedance magnitude, $|Z_x(\omega)|$, of an air column x. An oscillator produces a sinusoidal electrical signal which is amplified and used to drive a compression driver loudspeaker. The resultant acoustic signal passes through a cavity into a capillary. A microphone monitors the pressure $p_{\mathrm{cav}}(\omega)$ generated in the cavity. The microphone signal is amplified and passed back to a regulator which adjusts the oscillator output to ensure that the cavity pressure amplitude is maintained constant at all excitation frequencies; i.e. $|p_{\mathrm{cav}}(\omega)| = |p_{\mathrm{cav}}|$. The capillary is designed to have an impedance which is frequency independent, $Z_{\mathrm{cap}}(\omega) = Z_{\mathrm{cap}}$, and whose magnitude is much larger than that of the air column being measured; i.e. $|Z_{\mathrm{cap}}| \gg |Z_x(\omega)|$. Typically, the capillary in a measurement system of this type has an impedance magnitude of the order of $10^9\ \Omega$ [17, 18]. The capillary connects the cavity to a plate in which a microphone is embedded. The air column under test is mounted on the plate so that it is centred on the capillary with the microphone located approximately halfway between the centre and the edge of the air column; this minimises the effect of evanescent higher modes, generated at the cross-sectional discontinuity between the capillary and the air column, on the measurement of the plane wave component of the impedance

Document downloaded by @DAEL, 2026-11-17 20:35:34 - personal use only

[6, 19]. The microphone measures the pressure $p_x(\omega)$ at the entrance to the air column and the pressure amplitude is then plotted by a chart recorder. The chart recorder and the oscillator are coupled so that, as the frequency of the sine wave generated by the oscillator is increased, the tracer chart moves through the frequency range at the same rate resulting in a plot of pressure amplitude as a function of frequency. (It should be noted that with the addition of a phase meter, connected to the two microphones, it is also possible to extract information regarding the phase of the input impedance using this system.)

2.3. Constant volume velocity source

The design of the capillary, together with the cavity pressure feedback system, ensures a volume velocity source which has a constant amplitude over the frequency range of interest. This can be explained as follows.

The impedance of the series combination of capillary and air column can be expressed as the complex ratio of the pressure and volume velocity at the input to the capillary,

$$Z_{\text{cap}}(\omega) + Z_x(\omega) = \frac{p_{\text{cav}}(\omega)}{U_{\text{cav}}(\omega)}, \tag{7}$$

The volume velocity in the cavity, $U_{\text{cav}}(\omega)$, is the same as the volume velocity at the entrance to the air column, $U_x(\omega)$, except for a phase difference $\zeta(\omega)$. So, equation (7) can be rearranged to give

$$U_x(\omega) = \frac{p_{\text{cav}}(\omega)}{Z_{\text{cap}}(\omega) + Z_x(\omega)} \mathrm{e}^{\mathrm{j}\zeta(\omega)}. \tag{8}$$

Simplifying equation (8) by noting that $Z_{\text{cap}}(\omega) = Z_{\text{cap}}$ and $|Z_{\text{cap}}| \gg |Z_x(\omega)|$ gives

$$U(\omega) = \frac{p_{\text{cav}}(\omega)}{Z_{\text{cap}}} \mathrm{e}^{\mathrm{j}\zeta(\omega)}, \tag{9}$$

where the volume velocity is now denoted by $U(\omega)$ because it depends only on the cavity pressure and the properties of the capillary. That is, it is independent of the object being measured.

According to equation (9), both the amplitude and phase of the volume velocity vary with frequency. However, rewriting in terms of magnitude and incorporating the condition that $|p_{\text{cav}}(\omega)| = |p_{\text{cav}}|$ gives

$$\left| U \right| = \frac{\left| p_{\text{cav}} \right|}{\left| Z_{\text{cap}} \right|}. \tag{10}$$

The pressure amplitude in the cavity and the magnitude of the capillary impedance are both independent of frequency. Consequently, the volume velocity amplitude is also independent of frequency (and can be simply denoted by $|U|$).

2.4. Determination of input impedance magnitude

To convert a pressure amplitude versus frequency curve, produced by the measurement system described in section 2.2, to an impedance magnitude curve requires division by the volume velocity amplitude,

$$\left| Z_x(\omega) \right| = \frac{\left| p_x(\omega) \right|}{\left| U \right|}. \tag{11}$$

Because the volume velocity amplitude is the same whatever object is being measured, it can be found by carrying out a single calibration measurement. This normally involves using the measurement system to find the pressure amplitude at an arbitrary frequency for an object whose impedance is well predicted by theory.

For example, if calibration object a is a cylinder of length l and radius r, its impedance is [20, 21]

$$Z_a(\omega) = \frac{\rho c}{\pi r^2} \left[\frac{Z_{\text{load}} \pi r^2/(\rho c) + \mathrm{j} \tan(\underline{k} l)}{1 + \mathrm{j}[Z_{\text{load}} \pi r^2/(\rho c)] \tan(\underline{k} l)} \right], \tag{12}$$

where ρ is the density of air, $c = 331.6\sqrt{1 + T/273}$ is the speed of sound in air at temperature T, and $\underline{k} = k - \mathrm{j}\alpha$ is the complex propagation constant, with $k = \omega/c$ and

$$\alpha = \frac{\omega}{c} \left[\frac{1}{r} \sqrt{\frac{\eta}{2\omega\rho}} + \frac{\gamma - 1}{r} \sqrt{\frac{\kappa}{2\omega\rho c_p}} \right]$$

provided that the boundary-layer thickness is much less than the radius of the cylinder (which is the case for all of the calibration and test objects measured in this paper, over the frequency range investigated). Meanwhile, η is the coefficient of shear viscosity of air, c_p is the specific heat of air at constant pressure, κ is the thermal conductivity of air, and γ is the ratio of the principal specific heats of air. The load impedance is infinite if the cylinder is closed at the far end ($Z_{\text{load}} = \infty$) and is equal to the radiation impedance if the cylinder is open at the far end ($Z_{\text{load}} = 0.25(\rho c/\pi r^2)\underline{k}^2 r^2 + \mathrm{j}0.6(\rho c/\pi r^2)\underline{k} r$ provided that $kr \ll 1$, which again is the case for all of the calibration and test objects measured in this paper, over the frequency range investigated).

By measuring calibration object a using the capillary-based apparatus, the volume velocity amplitude can be found by dividing the measured pressure amplitude $|p_a(\omega)|$ by the theoretical impedance magnitude $|Z_a(\omega)|$ (obtained from equation 12),

$$\left| U \right| = \frac{\left| p_a(\omega) \right|}{\left| Z_a(\omega) \right|}. \tag{13}$$

Note that the volume velocity amplitude is frequency independent so the calibration measurement can be carried out at any arbitrary frequency.

Document downloaded by @DAEL, 2026-11-17 20:35:34 - personal use only

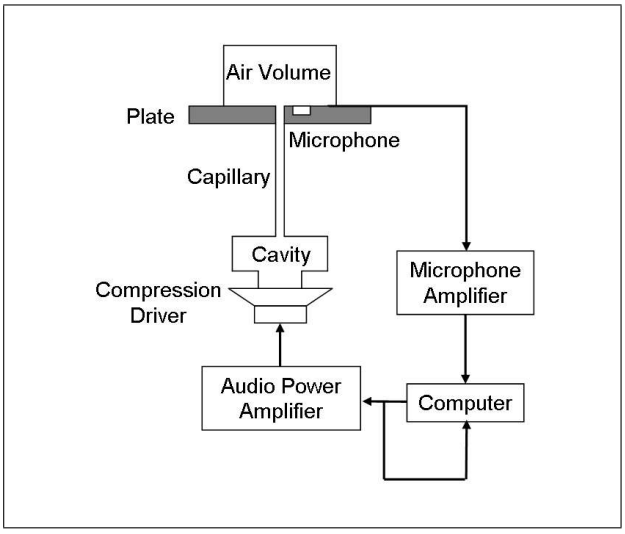


Figure 2. Modified single microphone capillary-based impedance measurement set-up.

3. Modified capillary-based measurement system

3.1. Introduction

In the basic capillary-based measurement system described in section 2.2, a microphone monitors the acoustic pressure in the cavity between the loudspeaker and the capillary. This microphone forms part of a feedback loop that maintains the cavity pressure constant, ensuring that the pressure amplitude recorded by a second microphone at the entrance to the air column under test is directly proportional to the input impedance magnitude. Phase information can also be obtained from the system through the use of a phase meter connected to the two microphones.

In this section, a modified capillary-based measurement set-up is reported in which the cavity microphone and associated feedback system have been removed. Even though the cavity pressure is no longer maintained constant during a measurement, the apparatus is still able to provide accurate values of input impedance magnitude. Moreover, despite only incorporating one microphone, the modified measurement set-up is also able to provide accurate measurements of input impedance phase.

3.2. Description of the measurement system

Figure 2 shows a schematic diagram of the modified single microphone capillary-based impedance measurement system. The system is controlled by a Windows-based PC containing a standard 16-bit sound card. The sound card is programmed (using the MATLAB software package with associated data acquisition toolbox) to play out a 50 Hz sinusoidal signal of 1V amplitude at an update rate of 44.1 kHz. The output of the sound card is amplified by a Cambridge Audio A1 stereo amplifier and used to drive a JBL 2426H compression driver loudspeaker. One hundred cycles of the electrical driving signal, $E_{ds}(\omega)$, are recorded on input channel 1 of the sound card using a sample rate of 44.1 kHz. As with the basic set-up described in section 2.2, the acoustic signal produced by the loudspeaker passes through a cavity into a capillary (in this case, comprising a 50 mm long, 2.6 mm diameter cylindrical tube with a solid hexagonal rod forced into it). However, in the modified set-up, there is no monitoring microphone positioned in the cavity and the cavity pressure amplitude is allowed to vary with frequency (due to the frequency response of the loudspeaker and the cavity resonances). The capillary is again intended to have a frequency independent impedance, Z_{cap}, whose magnitude is much larger than that of the air column being measured; i.e. $|Z_{\text{cap}}| \gg |Z_x(\omega)|$. The capillary connects the cavity to a plate in which a Knowles EK3132 electret microphone is embedded; the centre of the capillary and the centre of the microphone are separated by a distance of 5 mm. Again, to minimise the effect on the plane wave impedance measurement of evanescent higher modes generated in the region of the plate[1], the air column under test is mounted so that it is centred on the capillary; for most wind instruments, the microphone then lies approximately halfway between the centre and the edge of the mouthpiece. The microphone measures the pressure at the entrance to the air column. One hundred cycles of the voltage signal from the microphone, $E_x(\omega)$, are recorded on channel 2 of the sound card using a sampling frequency of 44.1 kHz. Note that the sound card simultaneously records both the driving signal sent to the loudspeaker and the signal from the microphone.

A Discrete Fourier Transform (DFT) is performed on the electrical driving signal recorded on channel 1 of the sound card. From this DFT, magnitude and phase spectra are calculated. As 100 cycles of the driving signal were recorded, the 101st frequency bin of the magnitude spectrum yields the amplitude of the driving signal $|E_{ds}(\omega)|$ averaged over the 100 cycles. Similarly, the 101st frequency bin of the phase spectrum yields the phase of the driving signal $\Phi_{ds}(\omega)$ averaged over 100 cycles. A similar procedure is performed on the microphone voltage signal recorded on channel 2 of the sound card, yielding the amplitude and phase of the microphone signal, $|E_x(\omega)|$ and $\Phi_x(\omega)$. By determining the amplitude and phase in this manner, the background noise contained in the other bins of the DFT is filtered out.

The amplitudes and phases of the driving signal and the microphone signal are stored on the PC. The entire measurement procedure is then repeated at 1 Hz intervals up to a frequency of 5 kHz. At each frequency, the phase of the voltage signal from the microphone is adjusted so that it is relative to that of the driving signal such that

$$E_x(\omega) = \left| E_x(\omega) \right| \mathrm{e}^{\mathrm{j}[\Phi_x(\omega) - \Phi_{ds}(\omega)]}. \tag{14}$$

[1] Although not used in this current work, recent papers [22, 23] describe correction terms that remove the error which is introduced into the measured plane wave impedance by the evanescent higher modes evoked at the discontinuity between capillary and air column. Another paper [24] suggests that, if the object used to calibrate the impedance measurement system has an entrance diameter equal to that of the air column under investigation, the generated higher modes are automatically taken into account.

Document downloaded by @DAEL, 2026-11-17 20:35:34 - personal use only

The pressure at the entrance of the air column is then

$$p_x(\omega) = M(\omega)E_x(\omega), \tag{15}$$

where $M(\omega)$ is the microphone response.

3.3. Determination of input impedance magnitude and phase

In the modified measurement system described in section 3.2, the feedback system has been removed and the cavity pressure amplitude is allowed to vary with frequency. Thus, the condition $|p_{\mathrm{cav}}(\omega)| = |p_{\mathrm{cav}}|$ no longer holds. Consequently, the volume velocity amplitude is no longer constant over the frequency range of interest; both the amplitude and the phase of the volume velocity vary with frequency. In principle, the removal of the feedback loop also means that the cavity pressure will have some dependence on the object being measured. However, the jump in impedance presented by the junction between the cavity and the capillary is so large that it can be reasonably assumed that any change in the cavity pressure arising when different objects are measured will be negligible.

For the moment, the capillary will still be assumed to have an impedance which is much greater than that of the object being measured. Under these circumstances, the volume velocity at the entrance to the air column is given by equation (9). It remains the same whatever object is being measured so is denoted $U(\omega)$. Providing this is the case, the complex impedance of the air column under test can be determined from a measured pressure amplitude versus frequency curve by performing a single calibration measurement to find $U(\omega)$.

3.3.1. Calibration procedure

The complex input impedance $Z_x(\omega)$ of an air column x measured using the modified system is the complex ratio of the pressure response $p_x(\omega)$ and the volume velocity $U(\omega)$ at the entrance to the air column,

$$Z_x(\omega) = \frac{p_x(\omega)}{U(\omega)}. \tag{16}$$

The principle employed to find the volume velocity is the same as described previously. The volume velocity is still independent of the object being measured. However, it now varies with frequency. The modified system is used to measure the complex pressure response $p_a(\omega)$ for a calibration object a whose impedance $Z_a(\omega)$ is well predicted by theory. For the calibration to be successful, the calibration object must, like the test object, have an impedance that is small compared with that of the capillary.

The volume velocity as a function of frequency is then found by dividing the measured complex pressure by the complex impedance at all frequencies in the range of interest,

$$U(\omega) = \frac{p_a(\omega)}{Z_a(\omega)}. \tag{17}$$

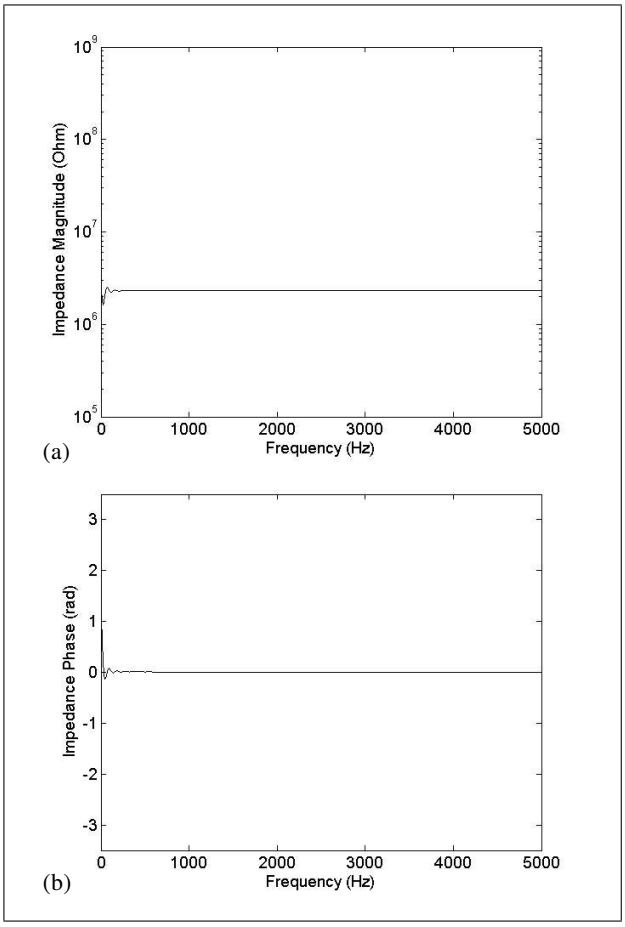


Figure 3. Theoretical input impedance curves for 50 m long open-ended cylindrical tube of radius 7.60 mm. (a) Magnitude and (b) Phase.

Combining equations (16) and (17) gives the following expression for the complex impedance of the test object:

$$Z_x(\omega) = \frac{p_x(\omega)}{p_a(\omega)} Z_a(\omega). \tag{18}$$

Substituting equation (15) into equation (18) then gives the complex impedance in terms of the recorded voltage signal from the microphone,

$$Z_x(\omega) = \frac{E_x(\omega)}{E_a(\omega)} Z_a(\omega). \tag{19}$$

The microphone response is eliminated from the equation and the input impedance of air column x can be calculated directly from the microphone voltage signals and the known theoretical impedance.

3.3.2. Results

The apparatus was calibrated using a 50 m long cylindrical tube of 7.60 mm radius that is open at the far end. Figure 3 shows theoretical impedance magnitude and phase curves for this calibration object (calculated using equation 12). It can be seen that, although there is some oscillation at low frequencies, the impedance magnitude and phase both remain essentially constant over the 50–5000 Hz frequency

Document downloaded by @DAEL, 2026-11-17 20:35:34 - personal use only

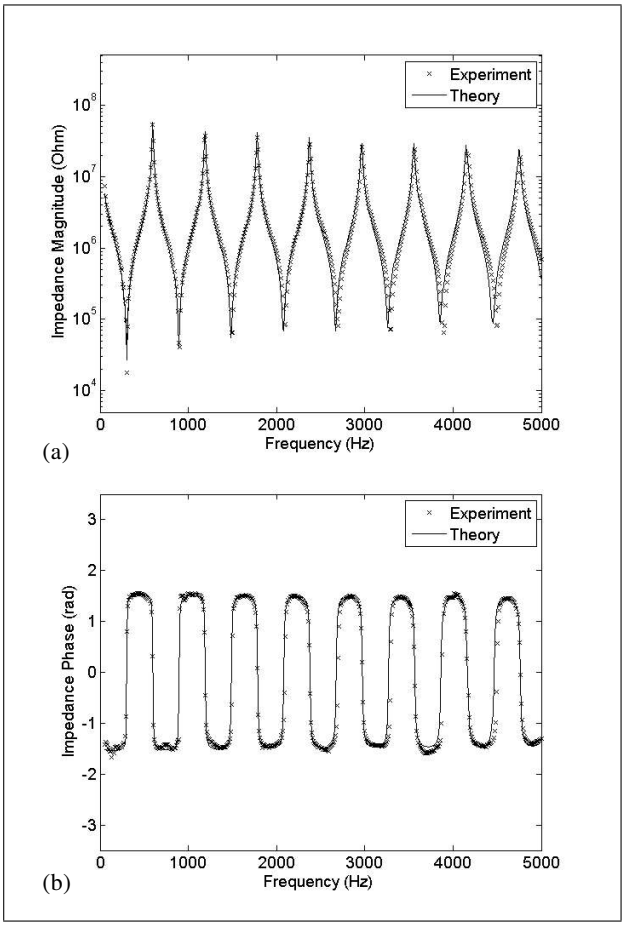


Figure 4. Measured and theoretical input impedance curves for 290 mm long closed cylindrical tube of radius 9.30 mm; measurement calibrated using 50 m long open-ended cylindrical tube of radius 7.60 mm. (a) Magnitude and (b) Phase.

range of interest. Choosing a calibration object whose impedance does not vary rapidly with frequency has several benefits. Firstly, it minimises the detrimental effect that any error in the value for the speed of sound used in equation (12) (such as might arise from small errors in the measurement of temperature and humidity) has on the accuracy of the calibration. Secondly, it helps to ensure that the variation in pressure amplitude recorded by the microphone during the calibration measurement remains well within the dynamic range of the sound card used in the measurement apparatus. Finally, it enables a good signal-to-noise ratio to be maintained at all frequencies during the calibration measurement. The use of resonance-free loads in the calibration of impedance measurement systems is discussed in detail in [10].

Figures 4a and 4b show measured impedance magnitude and phase curves for a 290 mm long cylindrical tube of radius 9.30 mm which is closed at the far end. For comparison purposes, theoretical impedance curves for the 290 mm tube (calculated using equation 12) are plotted alongside the measured curves. There is clearly a good agreement between the measured and theoretical impedance curves over the whole 50–5000 Hz range of interest. Indeed, for all eight peaks in the impedance magnitude curves, the difference between the experimentally measured and theoretically predicted values never exceeds 2.1 dB. A similarly good agreement is exhibited by the troughs in the impedance magnitude curves, with the exception of the first and seventh troughs (where the experimentally measured values are respectively 3.4 dB and 2.8 dB lower than the theoretically predicted values). Meanwhile, the measured phase curve follows the theoretical phase curve very closely, with just a small deviation between about 3600 and 3900 Hz. In terms of frequency, it is worth commenting that the measured magnitude curve lies slightly on the high frequency side of the theoretical magnitude curve. The most likely explanation for this is a small error in the value of the temperature used when calculating the theoretical curve (although all of the theoretical impedance curves presented in this paper are calculated using the temperature at which the associated impedance measurements were made, the thermometer used to monitor the temperature was only accurate to within ±0.5 °C).

The calibration object (the 50 m cylindrical tube) and the test object (the 290 mm cylindrical tube) used to generate the curves displayed in Figure 4 both have impedances that are small compared with that of the capillary. Providing this is the case, with a single calibration measurement, the modified capillary-based apparatus gives accurate measurements of both impedance magnitude and phase. However, the assumption that $|Z_{\mathrm{cap}}| \gg Z_x$ is not always true.

Figures 5a and 5b show measured impedance magnitude and phase curves for a stepped tube comprising a 2.10 mm long cylindrical section of radius 7.45 mm and a 303 mm long cylindrical section of radius 2.20 mm which is open at the far end. As with the measurements of Figure 4, the apparatus was calibrated using the 50 m tube of 7.60 mm radius. Again, for comparison purposes, theoretical impedance curves for the stepped tube are plotted alongside the measured curves. (These theoretical curves were calculated by using equation (12) to find the input impedance of the 303 mm long section and then treating this as the load impedance in a reapplication of equation (12) to find the impedance at the entrance to the 2.10 mm long section.) By comparing the measured curves with the theoretical impedance curves, it can be seen that the agreement is poorer than was observed in Figure 4. This is particularly apparent for the lowest frequency peaks in the impedance magnitude curves, with the measured values for the first four peaks smaller than the theoretically predicted values by 7.7 dB, 4.9 dB, 4.2 dB and 4.3 dB respectively. The reason for this discrepancy is that the impedance of the stepped tube, with its long narrow second section, is relatively high, rendering the assumption that $|Z_{\mathrm{cap}}| \gg Z_x$ invalid. Indeed, examination of the theoretical impedance magnitude curve reveals that the first four peaks have values in excess of $10^8\ \Omega$. Given that the capillary impedance in apparatus of this type is usually only of the order of $10^9\ \Omega$, it is clear that the assumption doesn't hold. As far as the impedance phase curves are concerned, there is a

Document downloaded by @DAEL, 2026-11-17 20:35:34 - personal use only

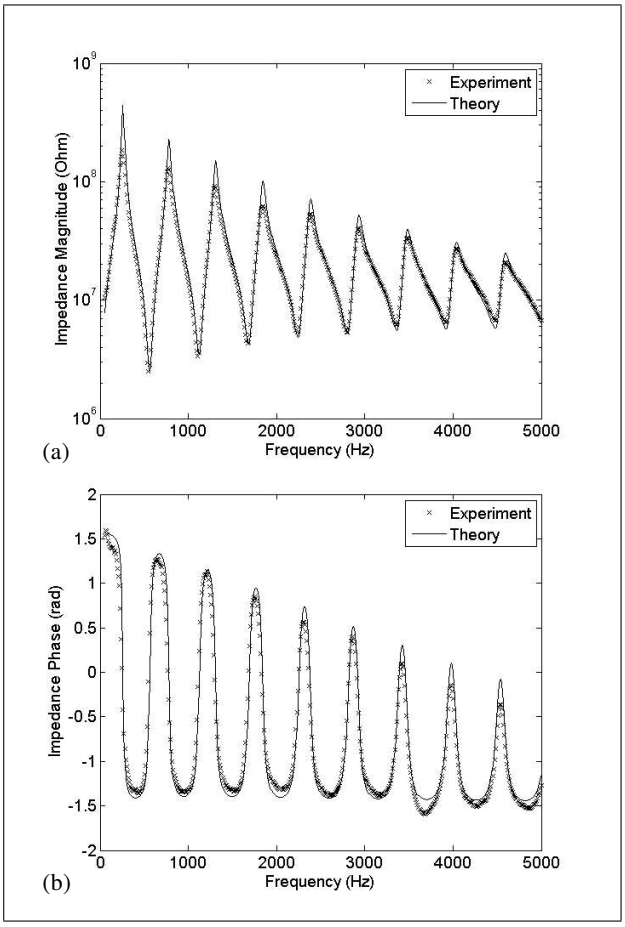


Figure 5. Measured and theoretical input impedance curves for test object comprising a 2.10 mm long cylindrical tube of radius 7.45 mm connected to a 303 mm long open-ended cylindrical tube of radius 2.20 mm; measurement calibrated using 50 m long open-ended cylindrical tube of radius 7.60 mm. (a) Magnitude and (b) Phase.

reasonable agreement between the measured and theoretical values at low frequencies. However, the agreement is less good as the frequency increases, with differences of as much as 0.3 radians observed above 3500 Hz.

4. Two calibration method

In this section, a method of calibration is described which enables accurate input impedance measurements to be made using the modified capillary-based apparatus, even when the impedance of the object under investigation is comparable in magnitude to that of the capillary. The method involves making measurements on two different objects whose impedances are well-known theoretically.

Although the two calibration method discussed here was developed specifically for calibrating the modified single microphone capillary-based system, it is closely related to the method used for calibrating the commercially available BIAS system [25, 26]. In fact, as the BIAS system contains two microphones (one in the cavity as well as one at the entrance to the object being measured), the method used when calibrating the BIAS system is more general than the method outlined in this section. Specifically, it doesn't rely on the assumption that the cavity pressure remains the same regardless of the object being measured (if this assumption were to be introduced, the method of calibrating the BIAS system would reduce to the calibration method that is described here for the single microphone capillary-based system). However, as discussed previously, the very large jump in impedance at the junction between the cavity and the capillary suggests that any loss of accuracy incurred by including this assumption will be minimal.

Following the description of the method, the improvement in accuracy that results from carrying out two calibration measurements is demonstrated experimentally through input impedance measurements both of the stepped tube described in the previous section and of a Boosey and Hawkes oboe.

4.1. Calibration procedure

If the assumption is removed that the capillary impedance is independent of frequency and much greater in magnitude than that of the object being measured, then the volume velocity is given by equation (8). It depends on the impedance of the air column and so changes depending on what object is being measured.

As the volume velocity is now affected by the presence of the air column, the expression for the complex impedance previously given by equation (16) must be rewritten,

$$Z_x(\omega) = \frac{p_x(\omega)}{U_x(\omega)}. \tag{20}$$

Combining equations (8) and (20) and rearranging gives an expression for the input impedance of the air column in terms of the pressure response, the capillary impedance and the cavity pressure,

$$Z_x(\omega) = \frac{p_x(\omega) Z_{\mathrm{cap}}(\omega)}{p_{\mathrm{cav}}(\omega) \mathrm{e}^{\mathrm{j}\zeta(\omega)} - p_x(\omega)}. \tag{21}$$

To find the complex impedance requires the capillary impedance and the cavity pressure to be measured. This can be done by carrying out two calibration measurements. When calibration object a is measured on the modified system, the volume velocity at the entrance to the air column is given by the following two equations:

$$U_a(\omega) = \frac{p_{\mathrm{cav}}(\omega)}{Z_{\mathrm{cap}}(\omega) + Z_a(\omega)} \mathrm{e}^{\mathrm{j}\zeta(\omega)}, \tag{22}$$

$$U_a(\omega) = \frac{p_a(\omega)}{Z_a(\omega)}. \tag{23}$$

Equating equations (22) and (23) and rearranging gives an expression for the cavity pressure,

$$p_{\mathrm{cav}}(\omega) = \frac{[Z_{\mathrm{cap}}(\omega) + Z_a(\omega)] p_a(\omega)}{Z_a(\omega)} \mathrm{e}^{-\mathrm{j}\zeta(\omega)}. \tag{24}$$

Document downloaded by @DAEL, 2026-11-17 20:35:34 - personal use only

Using a second calibration object b results in the following alternative expression for the cavity pressure:

$$p_{\mathrm{cav}}(\omega) = \frac{[Z_{\mathrm{cap}}(\omega) + Z_b(\omega)]p_b(\omega)}{Z_b(\omega)} \mathrm{e}^{-\mathrm{j}\zeta(\omega)}. \quad (25)$$

If it is once more assumed that the cavity pressure as a function of frequency is independent of the object being measured, equations (24) and (25) can be equated and rearranged to give the following expression for the capillary impedance:

$$Z_{\mathrm{cap}}(\omega) = \frac{Z_a(\omega)Z_b(\omega)[p_b(\omega) - p_a(\omega)]}{p_a(\omega)Z_b(\omega) - p_b(\omega)Z_a(\omega)}. \quad (26)$$

Substituting equations (24) and (26) into equation (21) gives the following expression for the input impedance of air column x:

$$Z_x(\omega) = \frac{p_x(\omega)Z_a(\omega)Z_b(\omega)\left[p_b(\omega) - p_a(\omega)\right]}{p_a(\omega)p_b(\omega)\left[Z_b(\omega) - Z_a(\omega)\right] + p_x(\omega)\left[p_b(\omega)Z_a(\omega) - p_a(\omega)Z_b(\omega)\right]}. \quad (27)$$

Using equation (15), the expression for the input impedance can be rewritten in terms of the microphone voltage signals when the unknown air column and the two calibration objects are measured,

$$Z_x(\omega) = \frac{E_x(\omega)Z_a(\omega)Z_b(\omega)\left[E_b(\omega) - E_a(\omega)\right]}{E_a(\omega)E_b(\omega)\left[Z_b(\omega) - Z_a(\omega)\right] + E_x(\omega)\left[E_b(\omega)Z_a(\omega) - E_a(\omega)Z_b(\omega)\right]}. \quad (28)$$

Again, the microphone response is eliminated from the equation and the input impedance of the air column can be determined from just the microphone voltage signals and the known theoretical impedances.

It should be noted that for the calibration to be successful, the two calibration objects must have different impedances but, more importantly, there also needs to be a significant difference in volume velocity between the two calibration measurements (the reason for this becomes apparent if the numerator and denominator of equation (27) are both divided by $Z_a(\omega)Z_b(\omega)$; when the difference in volume velocity is very small, the second term in the denominator tends to zero and the method reduces to the one calibration method). This can be ensured by using one calibration object whose impedance is much smaller than that of the capillary and one calibration object whose impedance is of comparable magnitude to that of the capillary. In addition, as was discussed in section 3.3.2, it is beneficial if the impedances of both calibration objects do not vary rapidly with frequency over the frequency range of interest.

4.2. Results

To calibrate the modified single microphone capillary-based system, the cylindrical tube of length 50 m and radius 7.60 mm was used as the first calibration object. As stated previously, the impedance of this tube is small compared with that of the capillary and remains relatively constant over the frequency range of interest. The second calibration object used consists of a short cylindrical section of length 1.00 mm and radius 9.30 mm connected to a cylindrical tube of length 30 m and radius 0.75 mm that is open at the far end. The first section is essentially a coupler to enable the calibration object to fit over the capillary and microphone of the measurement apparatus. Meanwhile, the narrow diameter of the second section of this object ensures an impedance that is non-negligible when compared with that of the capillary. Figure 6 shows theoretical impedance magnitude and phase curves for the second calibration object. As with Figure 3, the impedance of this calibration object doesn't exhibit any rapid variation with frequency and, therefore, the accuracy of the calibration measurement is maximised.

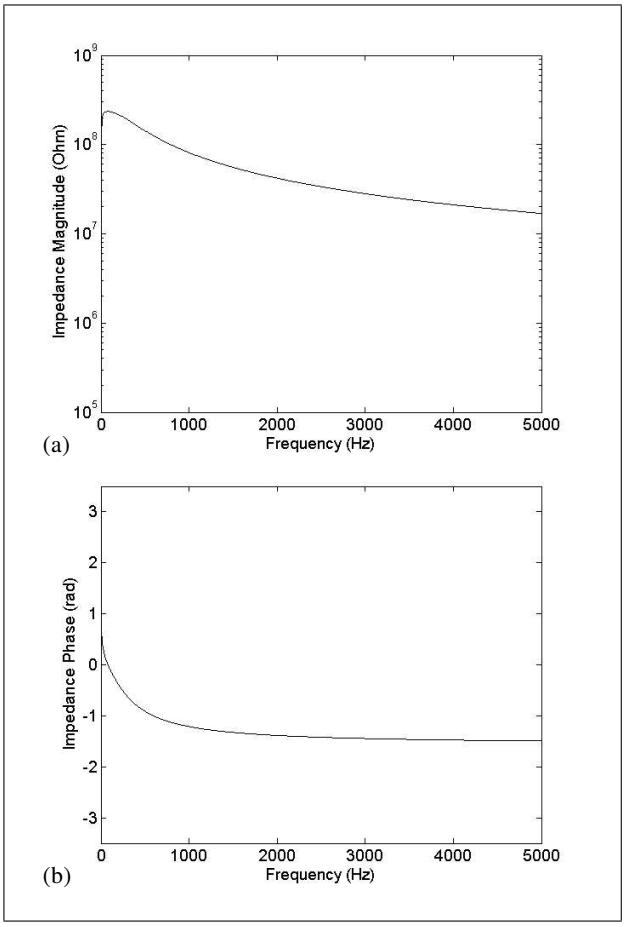


Figure 6. Theoretical input impedance curves for calibration object comprising 30 m long open-ended cylindrical tube of radius 0.75 mm with 1.00 mm long coupler of radius 9.30 mm. (a) Magnitude and (b) Phase.

Figures 7a and 7b show measured impedance magnitude and phase curves for the high impedance stepped tube (first introduced at the end of section 3.3.2) when the apparatus is calibrated using the two calibration objects described. As before, theoretical impedance curves for the stepped tube are plotted alongside the measured curves for comparison purposes.

Document downloaded by @DAEL, 2026-11-17 20:35:34 - personal use only

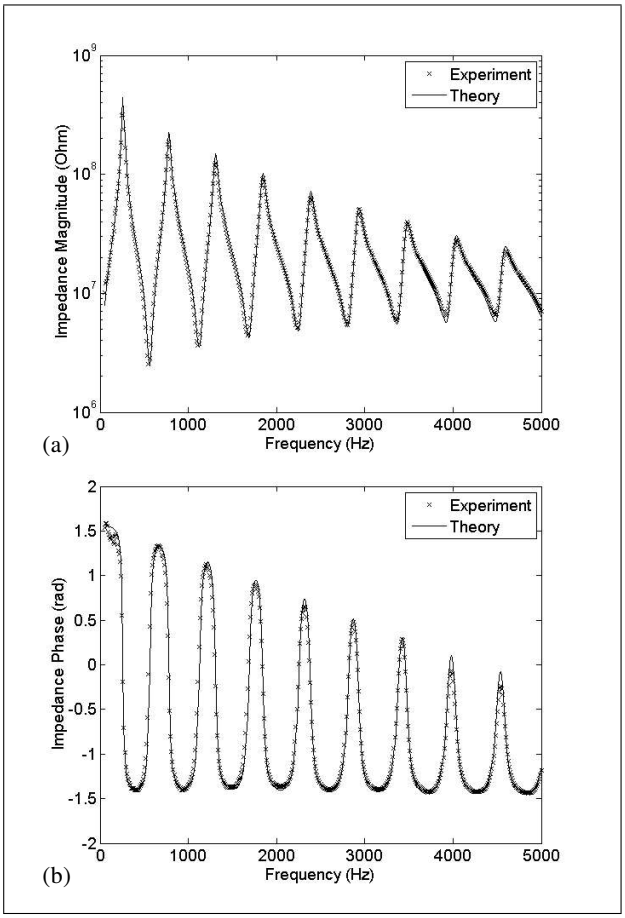


Figure 7. Measured and theoretical input impedance curves for test object comprising a 2.10 mm long cylindrical tube of radius 7.45 mm connected to a 303 mm long open-ended cylindrical tube of radius 2.20 mm; measurement calibrated using 50 m long open-ended cylindrical tube of radius 7.60 mm + 30 m long open ended tube of radius 0.75 mm with coupler. (a) Magnitude and (b) Phase.

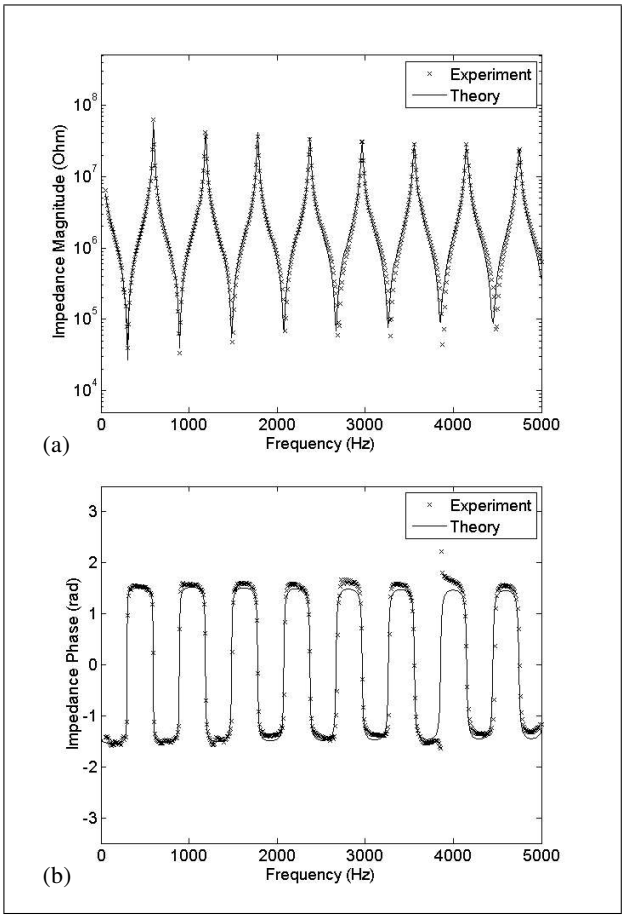


Figure 8. Measured and theoretical input impedance curves for 290 mm long closed cylindrical tube of radius 9.30 mm; measurement calibrated using 50 m long open-ended cylindrical tube of radius 7.60 mm + 30 m long open-ended tube of radius 0.75 mm with coupler. (a) Magnitude and (b) Phase.

Compared with Figure 5, there is now a much better agreement between the measured and theoretical impedance curves. Indeed, the difference between the measured value and the theoretical value for the first impedance magnitude peak is now only 2.9 dB, with a difference of less than 1.6 dB for all the other peaks. Similar levels of agreement are exhibited by the troughs in the impedance magnitude curves, with differences between experiment and theory of no greater than 1.2 dB. The accuracy of the measured magnitude curve is mirrored by the measured phase curve which follows the theoretically predicted curve very closely.

It is evident that the two calibration method provides a much more accurate impedance measurement of the high impedance stepped tube test object than that achieved using the standard one calibration measurement. The close match between the measured and theoretical curves of Figure 7 also indicates that the assumption that the cavity pressure does not change significantly when different objects are measured is reasonable. Of course, for the two calibration method to be universally applicable, it must also enable lower impedance test objects to be measured with a high level of accuracy. In order to investigate this, a measurement of the 290 mm long cylindrical tube has been carried out with the apparatus calibrated using the same two calibration objects. Figure 8a and Figure 8b show the resulting measured impedance magnitude and phase curves together with the corresponding theoretical curves. For all eight peaks in the impedance magnitude curves, the difference between the experimentally measured and theoretically predicted values never exceeds 1.3 dB (compared with the difference of 2.1 dB observed in Figure 4). However, the level of agreement exhibited by the troughs in the impedance magnitude curves is less good, with differences between the experimentally measured and theoretically predicted values of as much as 6.2 dB. Variations between the measured and theoretical impedance phase curves are also apparent at these frequencies. These errors in the experimentally measured values are a direct consequence of the large difference between the impedance of the second calibration object (the 30 m long open ended tube of radius 0.75 mm with coupler) and the impedance troughs of the 290 mm long closed tube. At the antiresonance frequencies of the 290 mm tube, this leads to the dif-

Document downloaded by @DAEL, 2026-11-17 20:35:34 - personal use only

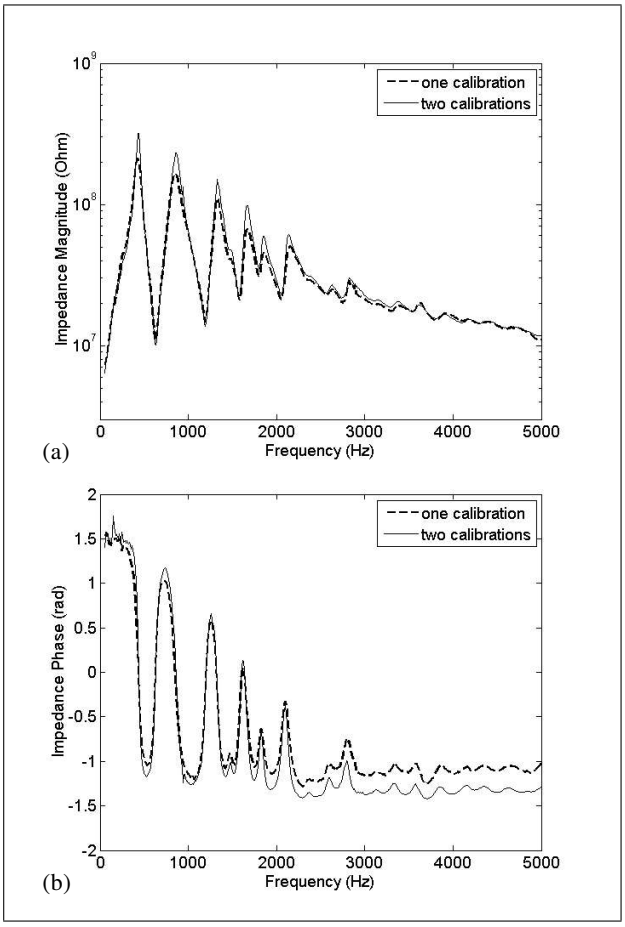


Figure 9. Measured input impedance curves for Boosey and Hawkes oboe with A4 fingering applied; measurements calibrated using 50 m long open-ended cylindrical tube of radius 7.60 mm (one calibration) and the same tube + 30 m long open-ended tube of radius 0.75 mm with coupler (two calibrations). (a) Magnitude (b) Phase.

ference between the pressure recorded during the second calibration measurement and that recorded during the test object measurement being too great for the dynamic range of the 16 bit sound card currently used in the measurement apparatus. Replacing this standard sound card with a dedicated data acquisition card that has a higher bit depth should therefore enable such dynamic range problems to be overcome.

As capillary-based systems of the type described in this paper are primarily used for measuring musical wind instruments, it is instructive to conclude this section by observing the effect of using a two calibration approach when measuring the input impedance of such an instrument. Figure 9 compares impedance magnitude and phase curves for a Boosey and Hawkes oboe (with A4 fingering applied) determined using both the one calibration method and the two calibration method. To make the measurements, a blank oboe staple (with the two pieces of reed cane removed) was inserted into the instrument. The oboe was then mounted on the apparatus via a bespoke coupler which connects the oboe staple to the microphone/capillary output via a 253 mm^3 volume, equivalent to that normally contained within the two pieces of reed cane.

It is clear from Figure 9a that using the one calibration method results in impedance magnitude peaks of lower amplitude than is the case when the two calibration method is used. Over the first six peaks, the difference ranges from 1.7 dB up to as much as 3.6 dB. Unsurprisingly, there is much better agreement between the one calibration and the two calibration methods with respect to the troughs in the impedance magnitude curves. Over the four discernible troughs, the difference never exceeds 0.7 dB. As far as the phase curves of Figure 9b are concerned, the two methods of calibration are in good agreement at low frequencies but, above around 1700 Hz, there is a difference of around 0.3 radians in the impedance phase measured by the two methods. This difference is similar to that observed at the higher frequencies between the theoretical and experimental curves of Figure 5b, when the high impedance stepped tube was measured using the one calibration method. Such a large difference was not observed in Figure 7b when the same stepped tube was measured using the two calibration method.

5. Conclusion

Although there are other more accurate techniques for determining acoustic impedance, the capillary-based approach remains the most widely used method of measuring the input impedance of musical wind instruments. With recent advances in data acquisition technology, and a reduction in the costs of computing hardware, it is now possible to produce an inexpensive single microphone capillary-based system that will run on a basic PC and provide both impedance magnitude and impedance phase measurements. Moreover, a two calibration approach (such as the one detailed in this paper or the one used for calibrating the BIAS system) provides a means of achieving more accurate impedance measurements using capillary-based apparatus. This improvement in accuracy is most noticeable when measuring high impedance objects. From the perspective of musical acoustics, it is therefore most significant when measuring instruments which have a narrow entrance to the air column, such as the oboe or the bassoon.

References

[1] J. C. Webster: An electrical method of measuring the intonation of cup-mouthpiece instruments. J. Acoust. Soc. Am. **19** (1947) 902–906.

[2] A. H. Benade: Physics of brasses. Scientific American (1973) 24–25.

[3] A. H. Benade: Fundamentals of musical acoustics. Dover, New-York, 1976.

[4] J. Backus: Input impedance curves for the reed woodwind instruments. J. Acoust. Soc. Am. **56** (1974) 1266–1279.

[5] J. Backus: Input impedance curves for the brass instruments. J. Acoust. Soc. Am. **60** (1976) 470–480.

[6] R. Caussé, J. Kergomard, X. Lurton: Input impedance of brass musical instruments. Comparison between experi-

Document downloaded by @DAEL, 2026-11-17 20:35:34 - personal use only

ment and numerical models. J. Acoust. Soc. Am. **75** (1984) 241–254.

[7] A. H. Benade, M. I. Ibisi: Survey of impedance methods and a new piezo-disk-driven impedance head for air columns. J. Acoust. Soc. Am. **81** (1987) 1152–1167.

[8] J.-P. Dalmont: Acoustic impedance measurement. Part 1: A review. Journal of Sound and Vibration **243** (2001) 427–439.

[9] M. van Walstijn, D. M. Campbell, J. A. Kemp, D. B. Sharp: Wideband measurement of the acoustic impedance of tubular objects. Acta Acustica united with Acustica **91** (2005) 590–604.

[10] P. Dickens, J. Smith, J. Wolfe: Improved precision in measurements of acoustic impedance spectra using resonance-free calibration loads and controlled error distribution. J. Acoust. Soc. Am. **121** (2007) 1471–1481.

[11] J.-P. Dalmont, J. C. Le Roux: A new impedance sensor for wind instruments. Acta Acustica united with Acustica **94** (2008) Suppl. 1, S46.

[12] M. Curtit, F. Yahaya, J.-P. Dalmont, J. Gilbert, O. Cottet: Bore reconstruction based on input impedance measurement: application to the bassoon crook. Proceedings of the Second Vienna Talk, University of Music and Performing Arts Vienna, Austria, Sept 19–21 2010.

[13] J. Kemp, M. van Walstijn, D. M. Campbell, J. Chick, R. Smith: Time domain wave separation using multiple microphones. J. Acoust. Soc. Am. **128** (2010) 195–205.

[14] G. Widholm, H. Pichler, T. Ossmann: BIAS: A computer-aided test system for brass wind instruments. An Audio Engineering Society Preprint, 1989, 2834.

[15] G. Widholm, W. Winkler: Evaluation of musical instrument quality by computer systems. Examples of realisation. Proceedings of the SMAC 93, Royal Swedish Academy of Music, ISBN: 91845289876, 1994, 560–565.

[16] G. Widholm: Brass wind instrument quality measured and evaluated by a new computer system. Proceedings of the 15th International Congress on Acoustics, Trondheim, 1995, III, 517–520.

[17] J. Backus: Acoustic impedance of an annular capillary. J. Acoust. Soc. Am. **58** (1975) 1078–1081.

[18] J. Kergomard, R. Causse: Measurement of acoustic impedance using a capillary: An attempt to achieve optimization. J. Acoust. Soc. Am. **79** (1986) 1129–1140.

[19] D. H. Keefe, A. H. Benade: Impedance measurement source and microphone proximity effects. J. Acoust. Soc. Am. **69** (1981) 1489–1495.

[20] L. E. Kinsler, A. R. Frey, A. B. Coppens, J. V. Sanders: Fundamentals of acoustics (3rd edition). John Wiley and Sons, 1982.

[21] D. E. Hall: Basic acoustics. John Wiley and Sons, 1987.

[22] D. Brass, A. Locke: The effect of the evanescent wave upon acoustic measurements in the human ear canal. J. Acoust. Soc. Am. **101** (1997) 2164–2175.

[23] N. H. Fletcher, J.Smith, A. Z. Tarnopolsky, J. Wolfe: Acoustic impedance measurements. Correction for probe geometry mismatch. J. Acoust. Soc. Am. **117** (2005) 2889–2895.

[24] V. Gibiat, F. Laloe: Acoustical impedance measurements by the two-microphone-three-calibration (TMTC) method. J. Acoust. Soc. Am. **88** (1990) 2533–2545.

[25] P. Anglmayer: Messung der akustischen Eingangsimpedanz von Blechblasinstrumenten. MSc thesis, Institute of Musical Acoustics, University of Music and Performing Arts Vienna, Austria, 2001.

[26] W. Kausel: Bore reconstruction of tubular ducts from acoustic input impedance curve. IEEE Transactions on Instrumentation and Measurement **53** (2004) 1097–1105.

Document downloaded by @DAEL, 2026-11-17 20:35:34 - personal use only